

Unpinned Schottky barrier formation at metal–GaAs interfaces

L. J. Brillson, R. E. Viturro, C. Mailhot, and J. L. Shaw
Xerox Webster Research Center, Webster, New York 14580

N. Tache, J. McKinley, and G. Margaritondo
Physics Department, University of Wisconsin, Madison, Madison, Wisconsin 53706

J. M. Woodall, P. D. Kirchner, G. D. Pettit, and S. L. Wright
IBM Thomas J. Watson Research Center, Yorktown Heights, New York 10598

(Received 3 February 1988; accepted 23 April 1988)

We have used soft x-ray photoemission spectroscopy measurements to demonstrate that metal–GaAs interfaces can exhibit relatively unpinned Fermi level (E_f) movements. For clean GaAs (100) surfaces obtained by molecular-beam epitaxy (MBE) growth and thermal decapping of a protective As overlayer, the metals Au, Al, Cu, and In produce a 0.6–0.7-eV range of E_f stabilization. For a given metal, this stabilization occurs at the same energies for *n*-type and *p*-type GaAs. Furthermore, E_f movements are metal-dependent and can evolve over multimonolayer coverages. These results are examined with respect to pronounced differences in semiconductor quality between MBE versus melt-grown GaAs and in the context of previous GaAs E_f measurements. A self-consistent analysis of the junction electrostatics accounts for the functional dependence of barrier height on metal work function. The results highlight the importance of bulk quality as well as interface specific phenomena in controlling the Schottky barrier formation at metal/III–V compound semiconductor interfaces.

I. INTRODUCTION

Schottky barrier formation at metal–GaAs interfaces has been studied extensively over the past two decades,^{1–3} both for its high-speed technological applications⁴ as well as its fundamental behavior in relation to the Schottky barrier formation of III–V compound semiconductors.^{5–7} It is a common and widely held belief that metal contacts to GaAs produce only a narrow band of Fermi level stabilization energies,^{2–15} regardless of the metal work function and that this behavior is representative of many metal–semiconductor interfaces, particularly those of III–V compound semiconductors.^{2,3,8–10} Efforts to account for this E_f “pinning” have produced a number of physical models including: (1) chemisorption-induced defect formation,^{10,13–15} (2) effective work function,¹⁶ (3) metal-induced gap states determined by semiconductor band structure,¹⁷ (4) metal-induced gap states due to metal bonding and/or interdiffusion with the semiconductor,^{18,19} (5) chemically induced dipoles,²⁰ and (6) virtual gap states combining aspects of (3) and (1).²¹ Over the past two years, surface science measurements of metals on the $\text{In}_x\text{Ga}_{1-x}\text{As}$ (100) ($0 \leq x < 1$) pseudobinary alloys,^{22,23} InAs (110),²³ and GaP (110)^{24,25} surfaces have revealed unpinned and even near-ideal, Schottky-like behavior. These results comprise a major part of the limited data base for clean metal/III–V compound semiconductor interfaces. In fact, examples of strong pinning appeared to be limited to GaAs and, to a lesser extent, InP.

We have now discovered that the metal–GaAs interface can exhibit relatively unpinned E_f movements. Metals on clean molecular-beam epitaxially (MBE) grown GaAs obtained by thermal decapping of a protective As overlayer^{22,23} exhibit a 0.6–0.7 eV (or larger) range of E_f stabilization. E_f stabilization occurs at the same energies for *n*- and *p*-type

GaAs, as expected from a self-consistent analysis of the junction electrostatics.^{26,27} Indeed, such an analysis reveals that the presence of an acceptor state with mid- 10^{13} cm^{-2} density at ~ 0.2 eV above the valence band edge is compatible with the dependence of measured Schottky barrier height on metal work function. Furthermore, E_f movements are metal-dependent and can evolve over multimonolayer coverages. Varying surface Ga-to-As ratios indicate that initial surface composition and reconstruction do not dominate the final metal/GaAs band bending. Previous work on clean, ordered GaAs interfaces without air exposure was based entirely on measurements of cleaved, melt-grown GaAs. We can now show that in general such material has orders-of-magnitude higher densities of deep trap levels than MBE-grown GaAs and that the energies of these levels are well-suited to account for room-temperature as well as low-temperature UHV interface pinning results. Recent cathodoluminescence measurements also show a contrast in deep levels present within the surface space charge region and reveal the electronic contributions of As-derived and metal-induced states at reduced bulk trap concentrations.²⁸ This interplay between As-derived, metal-induced, and bulk-trap-related states provides a straightforward explanation for past GaAs results, both melt- and MBE-grown, UHV as well as chemically treated. These results highlight the importance of bulk crystal quality as well as interface-specific phenomena in controlling the Schottky barrier formation of metal/III–V compound semiconductor interfaces.

II. EXPERIMENT

We performed soft x-ray photoemission spectroscopy (SXPS) measurements of the Ga and As core levels with metal deposition in order to monitor the GaAs E_f movements as the Schottky barriers formed. We measure bulk-

sensitive SXPS spectra of As 3*d* and Ga 3*d* core levels using $h\nu = 60$ and 40 eV, respectively, and surface-sensitive As 3*d* and Ga 3*d* core level spectra using 100 and 80 eV, respectively.²⁹ These energy sets produce photoelectrons with identical escape depth and thereby identical depth resolution for both elements. Comparison of bulk versus surface-sensitive spectra allow us to monitor E_f changes and band bending with metallization from rigid core level shifts (bulk-sensitive) versus any chemical shifts (surface-sensitive). Comparison of bulk versus surface-sensitive spectra provided a means to identify and separate effects due to chemical bonding changes. Failure to take this chemically shifted component into account can lead to erroneous values of band bending, particularly under low resolution conditions.

The initial Fermi level position relative to the valence band edge is determined by the valence band difference between the extrapolated leading edge of clean GaAs versus the midpoint of the leading edge of a thick Au film grounded to the photoelectron analyzer. Overall resolution of the core level spectra analyzed here is 0.23–25 eV for $h\nu = 40$ –60 eV and 0.26–0.37 eV for $h\nu = 80$ –100 eV. A valence band spectrum of a thick (100 Å) Au film deposited on a Ta substrate in contact with the GaAs established the initial E_f position of the clean semiconductor. Metal evaporation took place in an ultrahigh vacuum (UHV) chamber (base pressure $P = 8 \times 10^{-11}$ Torr) from W filaments with a pressure rise no higher than mid- 10^{-9} Torr. A quartz crystal oscillator near the semiconductor substrate monitored the thin film depositions.

In order to obtain clean, ordered GaAs (100) surfaces, we used MBE-grown GaAs films which were “capped” immediately after deposition with several hundred monolayers of “cracked” As as protection against ambient contamination. These caps were thermally desorbed in UHV to provide clean ordered surfaces, as determined by valence band (VB) photoemission and low-energy electron diffraction measurements. This desorption procedure involved several stages at temperatures up to 600 °C.²⁸ Desorption at the highest temperatures required only a few seconds, as determined from the rise and fall in chamber pressure. The 40 eV VB spectra exhibit a characteristic set of peak features which are particularly sensitive to ambient contamination and lattice disruption. Quantitative data on the LEED reconstruction are not yet available. Only a (1×1) pattern has been observed thus far.²³ We obtained characteristic valence band spectra for desorption times and temperatures which yield approximately stoichiometric surfaces from normalized core level intensities. For the specimens described here, GaAs layers 7500-Å thick ($n = 5 \times 10^{16}$ – 5×10^{17} Si cm⁻³ or $p = 1 \times 10^{18}$ Mg cm⁻³) were grown over 2000-Å thick GaAs ($n = 2 \times 10^{18}$ Si cm⁻³) and on top of an n^+ or p^+ GaAs substrate. This multilayer film structure yielded an unstrained GaAs (100) outer film and an Ohmic contact through the degenerately doped base layers and substrate.

III. RESULTS

We measured the band bending produced by deposition of Au, Al, Cu, and In on clean, ordered GaAs (100) surfaces under UHV conditions. The rigid Ga 3*d* and As 3*d* core lev-

el shifts observed by SXPS provided a measure of the band bending which occurred during the initial stages of Schottky barrier formation. Figure 1 shows Ga 3*d* and As 3*d* core level spectra for *p*-type GaAs under both bulk-sensitive [40 and 60 eV, respectively, in 1 (a)] and surface-sensitive [80 and 100 eV, respectively in 1 (b)] conditions as a function of increasing metal deposition. With initial metal deposition, both substrate Ga 3*d* peaks shift to lower kinetic energy,

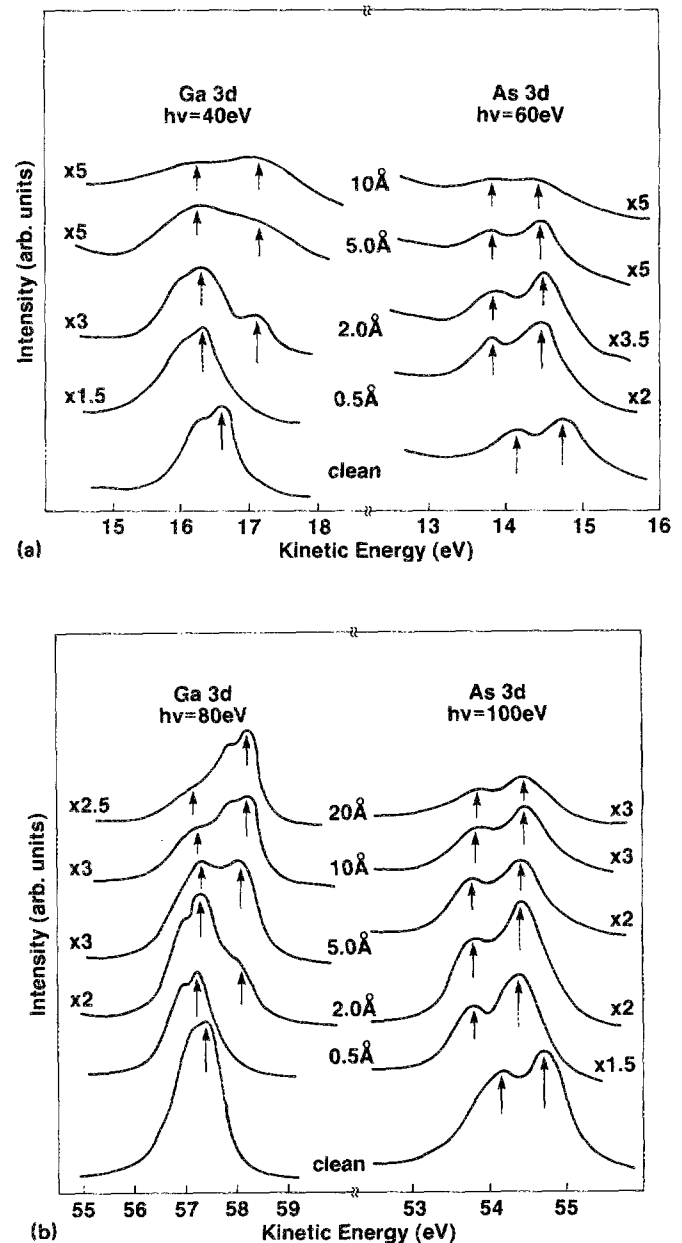


FIG. 1. Al/MBE-GaAs (100) *p* type. (a) Bulk and (b) surface-sensitive SXPS features for Ga 3*d* and As 3*d* core levels as a function of Al deposition on clean GaAs (100). Bulk-sensitive (40 eV) and surface-sensitive (80 eV) Ga 3*d* spectra both exhibit features due to substrate band bending and Ga dissociation. Bulk-sensitive Ga 3*d* and As 3*d* spectra in (a) exhibit rigid shifts due to band bending. The dissociated component dominates the features above 2 Å coverage in the surface-sensitive but not the bulk-sensitive spectra.

corresponding to increasing *p*-type (upward) band bending. A deposition of only 2 Å is sufficient to produce a second Ga 3*d* peak feature due to dissociated Al in both surface- and bulk-sensitive spectra. This feature continues to grow with increasing Al coverage and the splitting between dissociated and undissociated peaks increases. At coverages of 10–20 Å Al, the bulk-sensitive Ga 3*d* spectra still provides distinct energies for the substrate Ga while the surface-sensitive Ga 3*d* spectra reflect almost entirely the dissociated component. By considering only the undissociated Ga 3*d* component in the bulk-sensitive spectra, one obtains a 0.27 eV total band bending. A similar shift is apparent for the corresponding As 3*d* core level shown. Since the starting E_f position was $E_v + 0.53$ eV, E_f moves to 0.80 eV above E_{VBM} . We followed similar procedures in analyzing spectra for all other metals and GaAs surfaces reported here.

Figure 2 illustrates the E_f movements induced by deposition of Au, Al, Cu, and In on both *n*-type and *p*-type GaAs surfaces. The E_f behavior is strikingly different from that reported consistently for UHV-cleaved GaAs(110) surfaces. First, this set of common metals produce a range of E_f stabilization energies extending over 0.7 eV from $E_v + 0.18$ eV to $E_v + 0.92$ eV. This is in contrast to the narrow 0.2–0.25 eV range reported for GaAs (110)^{10,11} and GaAs (100)¹². Second, the E_f stabilization energies are the same for both *n*-type and *p*-type GaAs with the same metal. This is in contrast to the 0.2 eV separation seen for many adsorbates on UHV-cleaved GaAs (110).^{10,11,13} Third, the E_f stabilization occurs over 5–20 Å in all cases, and not within the sub-monolayer coverages reported for GaAs (110).^{10,11}

The GaAs specimens exhibit a range of 0.35 eV in E_f energies for their initial clean surfaces. The variation in starting

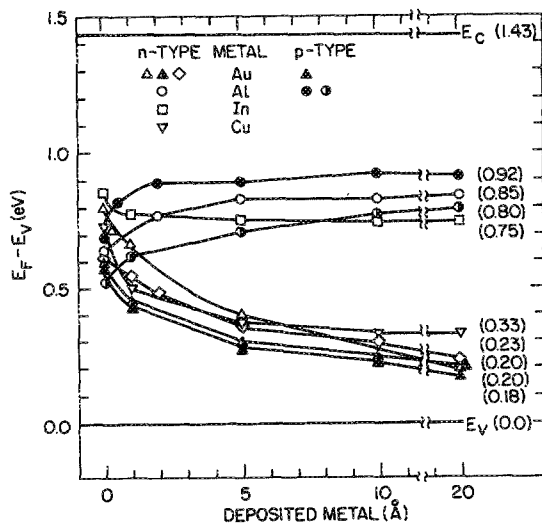


FIG. 2. Fermi level shifts within the GaAs band gap for deposition of Au, Al, In, and Cu on both *n*- and *p*-type GaAs (100) surfaces. The E_f shifts extend over 0.7 eV, are the same within experimental error (± 0.05 eV) for *n*- and *p*-type, and evolve over 5–20 Å coverages, depending on the metal. The initial E_f positions for clean, ordered GaAs are located in a 0.35 eV window near mid-gap.

energies may be related to differences in Ga:As stoichiometry, which is known to produce changes in E_f position.^{30,31} These variations correspond to reconstructions from (4×2) through (2×4) . However, significant differences in starting energies produce little or no differences in final stabilization energies, as evidenced by the Au and Al curves. For Au deposition on three *n*-type and one *p*-type surfaces, Fig. 2 shows an E_f stabilization range of 0.3 eV but a final E_f spread of only 0.05 eV after 20-Å deposition. Likewise, for Al deposition on one *n*-type and two *p*-type surfaces, Fig. 2 displays a 0.2 eV initial E_f range but a final E_f spread of only 0.12 eV. Thus the metal interaction rather than the starting surface appears to be dominant in determining final stabilization energies. This does not preclude compositional E_f effects caused by variations in Ga:As outdiffusion and resultant interfacial stoichiometry. Of primary significance, Fig. 2 demonstrates that metals on GaAs produce a wide range of E_f movements which is not constrained to a narrow window of mid-gap energies.

IV. DISCUSSION

Figure 3 illustrates the contrast between the band bending induced by metal deposition on clean MBE-grown GaAs(100) versus melt-grown GaAs(110) surfaces. Plotted versus metal work function Φ_M are barrier heights Φ_B (left ordinate) and E_f positions below the vacuum level (equal to barrier height Φ_B plus electron affinity X_{SC}) (right ordinate). Comparison of absolute valence band energies for UHV-cleaved (110) and thermally decapped (100) surfaces under identical conditions reveals the same binding

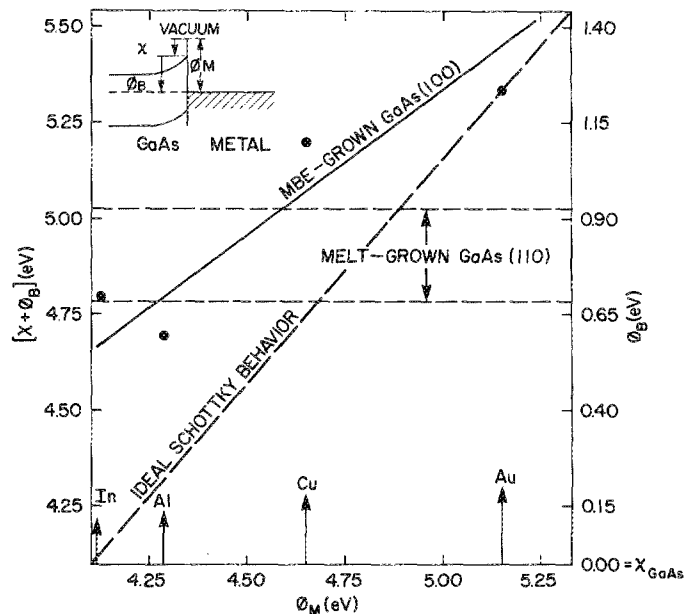


FIG. 3. GaAs barrier heights Φ_B and E_f positions below the vacuum level ($\Phi_B +$ electron affinity X_{SC}) plotted vs metal work function. Melt-grown GaAs (110) surfaces exhibit a 0.2–0.25 eV range near mid-gap for a wide variety of metals. Only four metals on MBE-grown GaAs (100) surfaces exhibit a 0.7 eV range which overlaps the melt-grown band and which extends to within 0.2 eV of the valence band. Ideal Schottky behavior appears in the upper left-hand inset and corresponds to the diagonal line.

for both orientations to within the precision of the SXPS energy measurements (± 0.05 eV). The inset in the upper left-hand corner represents ideal Schottky behavior and corresponds to the diagonal line shown. The melt-grown GaAs (110) surface exhibits a 0.2–0.25-eV range near mid-gap for a wide variety of metals. On the other hand, only four metals on MBE-grown GaAs (100) exhibit the 0.7-eV range found in Fig. 2. This 0.7-eV range overlaps the melt-grown band and extends to within 0.2 eV of the valence band edge. A line drawn through the four data points has a slope $S = 0.8$ eV vs $S \leq 0.25$ eV for the melt-grown data. However, only the Au data point lies on the $S = 1$ ideal Schottky line. This behavior indicates that the GaAs (100) surface, while permitting a wide range of Schottky barrier heights, still exhibits evidence for localized interface charge states.

The observation of nearly identical E_f positions for the same metal on both n -type and p -type GaAs is expected from a self-consistent electrostatic model of the interface E_f stabilization. For example, Zur *et al.*³² demonstrated that n -type and p -type GaAs approach a common energy asymptotically with interface energies in excess of 10^{14} donor and acceptor states cm^{-2} . The observation of a gap between n -type and p -type GaAs can be accounted for by a change in donor/acceptor character for the states localized at the metal–semiconductor interface.²⁶ Alternatively, the melt-grown experimental data may represent the energies before the interface has completely evolved.³²

In contrast to the melt-grown data, a self-consistent electrostatic analysis provides a simple picture of the interface state distribution required to account for the metal–GaAs (100) data. Figure 4 illustrates the results of such an analysis based on the generalized formalism of Duke and Mailhiot.^{26,27} Within this formalism, the energy positions, surface densities, and donor/acceptor characters of a set of interface states are varied to provide an optimal fit to the data points. The curves in Fig. 4 correspond to the dependence of barrier on work function for a single acceptor level located

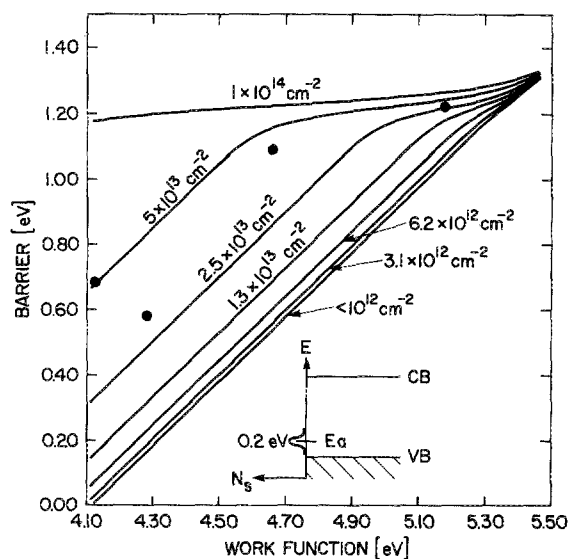


FIG. 4. Self-consistent electrostatic analysis of the metal/GaAs (100) data points. The generalized model of Duke and Mailhiot provides an optimal fit of interface state energies, densities of states, and donor/acceptor character.

0.2 eV above E_{VBM} with a selection of interface state densities. The data points from Fig. 3 lie between the ideal Schottky limit $N < 10^{12} \text{ cm}^{-2}$, and the strongly “pinned” limit $N \gg 10^{14} \text{ cm}^{-2}$. A single acceptor with density $N_A = 5 \times 10^{13} \text{ cm}^{-2}$ appears to fit the data most closely. Additional data points are required to narrow this density range further and to establish whether one or more charge states are involved.

Spectroscopic evidence is available which supports the existence of a modest density of states 0.2 eV above E_{VBM} . Viturro *et al.*²⁸ have obtained low-energy cathodoluminescence spectra for As-covered, clean, and Au-deposited GaAs (100) surfaces. These spectra show mid-gap features already present at 1.0 eV for the clean surface which are due to residual bulk traps. With deposition of 10 Å Au, two new features appear at 0.8 and 1.27 eV. The latter may correspond to optical transitions from the conduction band to a level 0.16 eV above E_{VBM} . Significantly, the densities of states proportional to these emissions are below that of the bulk trap emission, which in turn is at least two orders of magnitude below those found for UHV-cleaved, melt-grown GaAs (110) surfaces.²⁸ Thus the metal-induced features do not dominate the emission from states near the interface, consistent with the moderate density of states required by the analysis in Fig. 4. The additional feature at 0.8 eV bears a strong similarity to the additional state due to the As overlayer and may well be associated with an interface As accumulation linked to the Au–GaAs interdiffusion observed spectroscopically. Evidence for such accumulation is available from STEM measurements.³³

The barrier heights shown in Fig. 3 indicate much larger (smaller) barriers to n -type (p -type) GaAs than believed possible until now. Electrical measurements of GaAs prepared under nearly identical conditions have now begun and preliminary results indicate significantly higher barrier heights for Au than previously reported. Such electrical measurements of high barriers are complicated by the possible presence of multiple surface phases on a microscopic scale with different Schottky barriers, the lowest of which will reduce the overall barrier height disproportionately. Scanning tunneling microscopy measurements of ballistic charge injection are now available which yield evidence for such multiple phases with different barrier heights extending up to 1.1 eV.³⁴

Several factors can contribute to the pronounced difference in Schottky barrier formation for melt-grown versus MBE-grown GaAs. These include crystal surface orientation, excess As, thermal pretreatment, and bulk traps. Crystal orientation produces no major differences in deep levels for the relaxed GaAs (110)³⁵ vs (100)³⁶ clean surfaces. However, for adsorbates on GaAs, surface electronic structure calculations are available only for GaAs (110).³⁷ Such a comparison might reveal significant differences in surface relaxation and surface state density. However, to our knowledge, there exists no experimental evidence for significant barrier effects by crystal orientation alone. For example, barrier heights for melt-grown GaAs (100) surfaces¹² fall in the same narrow range as UHV-cleaved GaAs (110) surfaces.¹¹

Differences in growth conditions can lead to greater nonstoichiometries for the melt versus MBE-grown GaAs. For melt-grown GaAs, an As excess (typically fractions of a percent) is commonly employed to reduce dislocation densities in the crystal by orders of magnitude.³⁸ Metal contacts to such material can induce interdiffusion and/or reaction, resulting in an As segregation to the metal/GaAs interface which could be larger for melt versus MBE-grown material. Woodall and Freeouf have suggested¹⁶ that such excess As can stabilize Schottky barrier heights at a value consistent with the As work function and independent of metal work function. The CLS data of Viturro *et al.*²⁸ provides evidence to support the electrical activity of surface As and its presence at metal/GaAs interfaces. These CLS spectra show that Au deposition forms a state near mid-gap with 0.8-eV emission. This energy corresponds closely with the 0.8 eV feature evident on the As-capped surface and to the E_f position expected for the As work function (i.e., $\Phi_{As} = 4.8-5.0$ minus $X_{GaAs} = 4.1$). Furthermore, such a 0.8 eV feature is much more pronounced for CLS emission from melt-grown versus MBE-grown GaAs/metal interfaces, consistent with its typically higher bulk As composition. This link between metal-induced and As-related states is supported by chemical observations. For example, Au induces GaAs dissociation and nonstoichiometric As outdiffusion,³⁹⁻⁴¹ and such changes in interface stoichiometry can induce electrical activity with creation of interface chemical species (i.e., As inclusions, surface layers, and native defects).

The thermal pretreatment used to desorb the protective As cap (400–500 °C for several seconds to minutes) may also affect the MBE-grown surface. For example, such melt-grown treatment could reduce any As excess since As sublimates readily at elevated temperatures. GaAs annealed in vacuum also exhibits orders-of-magnitude reduced densities of native defects within microns of the surface.^{42,43} In particular, a thermal treatment at 675 °C for ~15 min leads to a reduction of the “EL2” defect and could be related to As surface loss.⁴²

A difference in the densities and energies of bulk traps can also account for Schottky barrier differences between melt versus MBE-grown GaAs. Indeed, they offer a relatively direct explanation consistent with the orders-of-magnitude higher densities of mid-gap levels observed via photoluminescence and cathodoluminescence spectroscopies. Melt-grown GaAs contains high concentrations of deep levels. For example, EL2 concentrations alone range up to 2×10^{16} cm⁻³ for liquid-encapsulated Czochralski (LEC)-grown⁴⁴ and to 5×10^{16} cm⁻³ for horizontal Bridgman (HB)-grown⁴⁵ GaAs, orders-of-magnitude higher than the 10^{13} cm⁻³ trap densities for MBE-grown GaAs.⁴⁶ Furthermore, LEC-grown crystals frequently contain native defects with the potential for electrical activity exceeding 10^{18} cm⁻³,⁴⁷ and melt-grown GaAs typically contains several electrically active deep levels, many of which have densities exceeding 10^{16} cm⁻³.⁴⁶ Finally, all of these electrically active sites have the potential to segregate to the GaAs surface,⁴⁸ thereby increasing the local deep level concentration. When such concentrations exceed the bulk doping, these interface traps can restrict E_f movement.³² This concept that high-state densi-

ties at GaAs interfaces are associated with crystalline defects in the surface space charge region is by no means novel, having been first suggested over 15 years ago.⁴⁹ The origin of such states may reside in the As-rich conditions under which they are grown, as already noted above, and the deep levels produced thereby.

Previous measurements of Schottky barriers for metals on MBE-grown GaAs support our E_f observations. Several groups have investigated the behavior of Al interfaces to GaAs (100) under high-vacuum conditions. Their barrier height and photoemission-derived E_f results indicate a significant range of E_f energies, ranging from 0.5 to 0.93 eV above E_{VBM} . See, for example, Refs. 30 and 50–54. The reported E_f positions for Al stabilization appear to be particularly sensitive to surface stoichiometry. The 0.85–0.86 eV position for Al shown in Fig. 1 agrees most closely with current–voltage ($J-V$) and ($C-V$) measurements for Al on As-rich surfaces.^{50,53} Our (1×1) LEED measurement of thermally decapped GaAs also suggests an As-rich surface.²³ For Au interfaces, our 0.18–0.21 eV value agrees with the only previous measurements available e.g., 0.2–0.3 eV above E_{VBM} from E_f measurements of a $c(4 \times 4)$ surface.⁵⁵ However, our value of 0.75 eV for In in Fig. 1 deviates from the single value of 0.93 eV above E_{VBM} reported from $J-V$ measurements.⁵⁴ To our knowledge, no data are available for comparison with our Cu measurement. Overall, previous measurements encompass the entire range of E_f positions shown in Fig. 1. (Interestingly, most researchers have concluded that previous results for metals on MBE-grown GaAs were analogous to melt-grown data, despite the larger range of E_f positions, and none appear to have recognized the relatively unpinned E_f behavior.) Moreover, data for Ge on MBE-grown GaAs suggest that the already large range of E_f movement may extend even closer to the conduction band edge.⁵⁶

Previous data for metals on MBE-grown and melt-grown GaAs(100) surfaces do not support a strong dependence of E_f stabilization on either thermal processing or crystal orientation alone. Previous results for Al^{30,50,51} and Au⁵⁵ do not seem to depend strongly on the thermal treatment alone prior to metallization.¹² Likewise, the narrow range of barriers measured for metals on melt-grown GaAs (100) surfaces¹² argues against a major influence of crystal orientation, notwithstanding any residual contamination, nonstoichiometry, or lattice damage following thermal cleaning of the air-exposed surface. On the other hand, Ge and Si deposition on to heated, melt-grown (100) substrates produces a much wider E_f range.⁵⁷ Further tests of crystal orientation and thermal effects include As capping and thermal desorption of clean, melt-grown GaAs (100) surfaces as well as annealing of UHV-cleaved GaAs (110) surfaces and are in progress.

Differences in bulk trap densities may well explain the temperature-dependent E_f stabilization behavior reported for various metals on melt-grown GaAs (110) surfaces.⁵⁸ PL measurements of melt-grown GaAs reveal not only a relatively high density of mid-gap states near the final pinning energies, but also the presence of a lower density of states with emission at 1.15 eV (1.06 eV at room temperature).²⁸

Assuming this emission is referenced to the the valence band edge, then the activation of such deep levels can strongly retard changes in population and band bending as charge transfers to a metal contact, especially at low temperature. Such a retardation in band bending occurs at almost exactly this energy at low temperature.⁵⁸ Since the density of this level is at least two orders of magnitude larger than any such level in MBE-grown GaAs, a test of this hypothesis will be to compare the low-temperature E_f behavior of MBE to melt-grown material.

V. IMPLICATIONS FOR SCHOTTKY BARRIER MODELS

The E_f measurements described here provide clear evidence for unpinned metal–GaAs interfaces. The large range of Schottky barrier heights for MBE-grown GaAs(100) surfaces indicates that any states induced by chemisorption or chemical interdiffusion play only a secondary role in the E_f stabilization. For melt-grown GaAs, the existence of high densities of states near mid-gap provides a direct explanation for the rapid E_f movements to a correspondingly narrow energy range reported previously.^{10,13} Metal-induced gap states (MIGS),¹⁷ virtual-induced gap states (VIGS),²¹ disorder-induced gap states (DIGS),⁵⁹ and other pinning models are not relevant to GaAs since, outside of the melt-grown material, a wide range of E_f movement is in fact present. This last observation is therefore fully compatible with the results afforded by the analyses of Refs. 26 and 27, which indicate that atomic (rather than electronic) relaxation/reaction are responsible for the observed insensitivity of rectifying barrier height to metal work function. The failure of MIGS-type models could in principle be due to chemically distinct interface layers produced by diffusion or reaction which can alter the proposed metal wave function tailing into the semiconductor. Such layers would severely limit the utility of these models since chemical interactions are evident for most metal/semiconductor interfaces.^{5,6}

The E_f results in Figs. 1 and 2 are consistent with a larger role of interfacial As in stabilizing the melt-grown versus MBE-grown GaAs/metal interface. The electrical activity of interfacial As is evident in CLS spectra of Viturro *et al.*²⁸ and a comparison of melt versus MBE-grown GaAs CLS spectra suggests that discrete, As-related states¹⁶ play a larger role in the former. Finally, when taken with previous results for InAs, InGaAs, and GaP, the results presented here for MBE-grown GaAs demonstrate that E_f pinning of metal–semiconductor interfaces in a narrow energy range, irrespective of the metal, is not characteristic of III–V compound semiconductors.

The results presented in Fig. 3 show that a Schottky formalism is capable of providing self-consistent results for the interface electrostatics. These results support the conclusion that interface dipoles are negligibly small at metal–semiconductor interfaces in the absence of extrinsic charge states (i.e., due to impurities, native defects, chemisorption, reaction, diffusion, nonstoichiometry, etc.), as calculated by Duke and Mailhot.^{26,27} Thus, the results of modern surface science experiments on clean, high-quality, metal–semiconductor interfaces should in general be amenable to such a

self-consistent electrostatic analysis.

The need to understand and control Schottky barrier formation has been a driving force for basic research into mechanisms of E_f pinning for many years. (Indeed the Schottky model itself is now 50 years old.^{60,61}) While E_f pinning on melt-grown GaAs will likely continue to be a controversial issue, it appears not to be a major one for MBE-grown GaAs(100) surfaces. Fortunately, the latter are prime candidates for future high-speed device structures. With the large range of barrier heights now available for III–V compound semiconductors, the main focus of interface barrier research may perhaps shift from a search for mechanisms to account for pinning to methods of semiconductor growth and processing which afford even greater control.

VI. CONCLUSIONS

We have demonstrated that a wide range (0.7 eV or more) of Schottky barrier heights exists for metals on GaAs (100) surfaces grown by MBE. Metals on *n*-type and *p*-type GaAs yield nearly identical E_f stabilization positions, in agreement with self-consistent electrostatic calculations. The Schottky barriers evolve over monolayers and depend in detail on the particular metal overlayer. These results contrast sharply with analogous measurements for metals on melt-grown GaAs. Our results are consistent with previous reports for individual MBE-grown GaAs/metal contacts. These results highlight the importance of bulk crystal quality as well as interface-specific phenomena in controlling Schottky barrier formation of metal III–V compound semiconductor interfaces.

ACKNOWLEDGMENTS

Partial support by the Office of Naval Research (Grant No. ONR N00014-80-C-0778), the Army Research Office (Contract DAAL03-86-C-003) and fruitful discussions with C. B. Duke, J. Lagowski, and H. H. Wieder are gratefully acknowledged. We also wish to thank the staff of the Sychrotron Radiation Center of the University of Wisconsin-Madison, which is supported by the National Science Foundation.

¹A. M. Cowley and S. M. Sze, *J. Appl. Phys.* **36**, 3212 (1965).

²S. M. Sze, *Physics of Semiconductor Devices*, 2nd ed. (Wiley-Interscience, New York, 1981), Chap. 5, pp. 274–297.

³See also, *Proceedings of the Physics of Compound Semiconductor Interfaces*, 1976–1981 and the *Physics and Chemistry of Semiconductor Interfaces*, 1982–present (American Institute of Physics, New York, NY).

⁴D. K. Ferry, *Gallium Arsenide Technology* (Howard W. Sams, Indianapolis, IN, 1985).

⁵L. J. Brillson, *Surf. Sci. Rep.* **2**, 123 (1982), and references therein.

⁶G. Margaritondo, *Solid State Electron.* **26**, 499 (1983).

⁷W. E. Spicer and W. E. Eglash, in *VLSI Electronics: Microstructure Science* (Academic, New York, 1985), Vol. 10, p. 79.

⁸C. A. Mead, *Solid State Electron.* **9**, 1023 (1966).

⁹S. Kurtin, T. C. McGill, and C. A. Mead, *Phys. Rev. Lett.* **22**, 1433 (1970).

¹⁰W. E. Spicer, I. Lindau, P. Skeath, C. Y. Su, and P. Chye, *Phys. Rev. Lett.* **44**, 420 (1980).

¹¹N. Newman, W. E. Spicer, T. Kendelewicz, and I. Lindau, *J. Vac. Sci. Technol. B* **4**, 931 (1986).

¹²J. R. Waidrop, *Appl. Phys. Lett.* **44**, 1002 (1984).

- ¹³W. E. Spicer, I. Lindau, P. Skeath, and C. Y. Su, *J. Vac. Sci. Technol.* **17**, 1019 (1980).
- ¹⁴R. H. Williams, R. R. Varma, and V. Montgomery, *J. Vac. Sci. Technol.* **16**, 1418 (1979).
- ¹⁵H. H. Wieder, *J. Vac. Sci. Technol.* **15**, 1498 (1978).
- ¹⁶J. M. Woodall and J. L. Freeouf, *J. Vac. Sci. Technol.* **19**, 794 (1981); J. L. Freeouf and J. M. Woodall, *Appl. Phys. Lett.* **39**, 727 (1981).
- ¹⁷J. Tersoff, *Phys. Rev. B* **32**, 6968 (1985).
- ¹⁸R. Ludeke, D. Straub, F. J. Himpsel, and E. Landgren, *J. Vac. Sci. Technol. A* **4**, 874 (1986).
- ¹⁹L. J. Brillson, in *Proceedings of the Thirteenth International Conference on the Physics of Semiconductors*, edited by F. G. Fumi (Typografica Marves, Rome, 1976), p. 665; *Phys. Rev.* **18**, 2431 (1978).
- ²⁰L. J. Brillson, *J. Vac. Sci. Technol.* **16**, 1137 (1979).
- ²¹W. Mönch, *Phys. Rev. Lett.* **58**, 1360 (1987).
- ²²L. J. Brillson, M. L. Slade, R. E. Viturro, M. Kelly, N. Tache, G. Margaritondo, J. M. Woodall, G. D. Pettit, P. D. Kirchner, and S. L. Wright, *Appl. Phys. Lett.* **48**, 1458 (1986).
- ²³L. J. Brillson, M. L. Slade, R. E. Viturro, M. Kelly, N. Tache, G. Margaritondo, J. Woodall, G. D. Pettit, P. D. Kirchner, and S. L. Wright, *J. Vac. Sci. Technol. B* **4**, 919 (1986).
- ²⁴L. J. Brillson, R. E. Viturro, M. L. Slade, P. Chiaradia, D. Kilday, M. Kelly, and G. Margaritondo, *Appl. Phys. Lett.* **50**, 1379 (1987).
- ²⁵P. Chiaradia, R. E. Viturro, M. L. Slade, L. J. Brillson, D. Kilday, M. Kelly, N. Tache, and G. Margaritondo, *J. Vac. Sci. Technol. B* **5**, 1075 (1987).
- ²⁶C. B. Duke and C. Mailhot, *J. Vac. Sci. Technol. B* **3**, 1970 (1985).
- ²⁷C. Mailhot and C. B. Duke, *Phys. Rev. B* **33**, 1118 (1986).
- ²⁸R. E. Viturro, J. L. Shaw, C. Mailhot, N. Tache, J. McKinley, G. Margaritondo, J. M. Woodall, P. D. Kirchner, G. D. Pettit, S. L. Wright, and L. J. Brillson (unpublished).
- ²⁹M. P. Seah and W. A. Dench, *Surf. Interface Anal.* **1**, 2 (1979).
- ³⁰S. P. Svensson, J. Kanski, T. G. Andersson, and P. O. Nilsson, *J. Vac. Sci. Technol. B* **2**, 235 (1984).
- ³¹R. Z. Bachrach, R. S. Bauer, P. Chiaradia, and G. V. Hansson, *J. Vac. Sci. Technol.* **18**, 797 (1981).
- ³²A. Zur, T. C. McGill, and D. L. Smith, *Phys. Rev. B* **28**, 2060 (1983).
- ³³Z. Liliental-Weber, *J. Vac. Sci. Technol. B* **5**, 1007 (1987).
- ³⁴W. J. Kaiser and L. D. Bell (unpublished).
- ³⁵D. J. Chadi, *J. Vac. Sci. Technol.* **15**, 1244 (1978); *Phys. Rev. B* **18**, 1800 (1987).
- ³⁶D. J. Chadi, *J. Vac. Sci. Technol. A* **5**, 834 (1987).
- ³⁷D. J. Chadi and R. Z. Bachrach, *J. Vac. Sci. Technol.* **16**, 1159 (1979).
- ³⁸J. C. Bryce and G. D. King, *Nature* **209**, 1346 (1966).
- ³⁹R. Z. Bachrach and A. Bianconi, *J. Vac. Sci. Technol.* **15**, 525 (1978).
- ⁴⁰P. W. Chye, I. Lindau, P. Pianetta, C. M. Garner, C. Y. Su, and W. E. Spicer, *Phys. Rev. B* **18**, 5545 (1978).
- ⁴¹L. J. Brillson, G. Margaritondo, and N. G. Stoffel, *Phys. Rev. Lett.* **44**, 667 (1980).
- ⁴²S. Makram Ebeid, D. Gautard, P. Devillard, and G. M. Martin, *Appl. Phys. Lett.* **40**, 161 (1982).
- ⁴³M. Matsui and T. Kazuno, *Appl. Phys. Lett.* **51**, 658 (1987).
- ⁴⁴D. E. Holmes, R. Y. Chen, K. R. Elliot, and C. G. Kirkpatrick, *Appl. Phys. Lett.* **40**, 46 (1982).
- ⁴⁵J. Lagowski, H. C. Gatos, J. M. Parsey, K. Wada, M. Kaminska, and W. Walukiewicz, *Appl. Phys. Lett.* **40**, 342 (1982).
- ⁴⁶A. Mirceau and D. Bois, *Inst. Phys. Conf. Ser.* **46**, 82 (1979).
- ⁴⁷I. Fujimoto, *Jpn. J. Appl. Phys.* **23**, L287 (1984).
- ⁴⁸A. Yakata and M. Nakajima, *Jpn. J. Appl. Phys.* **23**, L313 (1984).
- ⁴⁹T. M. Valahas, J. S. Sochanski, and H. C. Gatos, *Surf. Sci.* **26**, 41 (1971).
- ⁵⁰S. P. Svensson, G. Landgren, and T. G. Andersson, *J. Appl. Phys.* **54**, 4474 (1983).
- ⁵¹A. Y. Cho and P. D. Dernier, *J. Appl. Phys.* **49**, 3328 (1978).
- ⁵²W. I. Wang, *J. Vac. Sci. Technol. B* **1**, 574 (1983).
- ⁵³D. C. Sun, H. Sakaki, H. Ohno, Y. Sekeguchi, and T. Tanoue, *Inst. Phys. Conf. Ser.* **63**, 311 (1982).
- ⁵⁴K. Okamoto, C. E. C. Wood, and L. F. Eastman, *Appl. Phys. Lett.* **38**, 636 (1981).
- ⁵⁵K. L. I. Kobayashi, N. Watanabe, T. Narusawa, and H. Nakashima, *J. Appl. Phys.* **58**, 3758 (1985).
- ⁵⁶P. Chiaradia, A. D. Katnani, H. W. Sang, Jr., and R. S. Bauer, *Phys. Rev. Lett.* **52**, 1246 (1984).
- ⁵⁷R. W. Grant and J. R. Waldrop, *J. Vac. Sci. Technol. B* **5**, 1015 (1987).
- ⁵⁸K. Stiles, A. Kahn, D. G. Kilday, and G. Margaritondo, *J. Vac. Sci. Technol. B* **5**, 987 (1987).
- ⁵⁹H. Hasagawa and T. Sawada, *Thin Solid Films* **103**, 119 (1983).
- ⁶⁰B. Davidov, *J. Tech. Phys. USSR* **5**, 87 (1938).
- ⁶¹W. Schottky, *Z. Phys.* **113**, 367 (1939).